Acta Cryst. (1991). **B47**, 210–216

Sodium-Ion Distribution in Na^+ β-Alumina: a Crystallographic Challenge

By Kristina Edström and John O. Thomas

Institute of Chemistry, University of Uppsala, Box 531, *S*-751 21 *Uppsala, Sweden*

and Gregory C. Farrington

*Department of Materials Science and Engineering K*1, *University of Pennsylvania, Philadelphia, PA* 19104, *USA*

(*Received* 29 *May* 1990; *accepted* 31 *October* 1990)

Abstract

The Na^+-ion distribution in Na^+ β-alumina has been reinvestigated at 295 K by conventional single-crystal X-ray diffraction techniques (Mo $K\bar{\alpha}$ radiation, $\lambda = 0{\cdot}71073$ Å). The structure [idealized formula: $Na_{1+x}Al_{11}O_{17+x/2}$ for $x = 0{\cdot}22$, $M_r = 598{\cdot}6$, $F(000) = 586{\cdot}6$] comprises spinel-type blocks interleaving two-dimensional conduction planes with a spacing of ~ 11 Å. The atoms in the spinel framework have the centrosymmetric hexagonal space group $P6_3/mmc$ with $a = 5{\cdot}5929$ (4), $c = 22{\cdot}526$ (3) Å, $V = 610{\cdot}22$ Å^3, $Z = 2$, $D_x = 3{\cdot}25$ g cm^{-3}, $\mu_o = 10{\cdot}3$, $\mu_c = 10{\cdot}3$ cm^{-1}. The Na^+-ion distribution within the conduction plane is described using three different models: the best fit is obtained for a model in which the Na^+ ions occupy Beevers–Ross and interstitial sites near mid-oxygen, Na(1) and Na(2), respectively, $wR(F^2) = 0{\cdot}0436$ for 2036 observed reflections. Thermal vibration and/or displacement is described with β_{ij} and γ_{ijk} tensors for Na(1), and β_{ij} tensors only for Na(2). Neither the inclusion of additional Na^+ sites, nor the removal of the mirror-plane constraint on the conduction plane (to test for local ordering) could be shown to bring about significant improvement to the model. Attempts to refine local ordering within the Frenkel defect were also made with negative results. The crystallographic result is discussed in terms of possible conduction mechanisms.

Introduction

The ionic conductor Na^+ β-alumina has been studied extensively since the discovery in 1967 of its high Na^+-ion conductivity (Yao & Kummer, 1967). Interest has, for many years, focussed on the possibility of using the compound as a solid electrolyte in high-temperature batteries. More recently, however, the compound has also served as a model for studying such fundamental phenomena as ion–ion correlation effects and ion-exchange mechanisms. This work has exploited the geometrical simplicity of the channels provided for the mobile ions by the rigid spinel host.

The structure of Na^+ β-alumina has been studied many times. The first serious structure determination was made by Bragg, Gottfried & West (1931). At that time, the non-stoichiometry of the compound was not fully appreciated, which led to some spurious conclusions. Within the assumed space group, the compound appeared to contain more sodium than was observed by chemical analysis. Bragg *et al.* (1931) suggested some degree of disorder in the structure. A few years later, Beevers & Ross (1937) returned to a description in terms of the ideal stoichiometric formulation $NaAl_{11}O_{17}$. This work was based on a more reliable chemical analysis. The Na^+ ions were proposed to occupy 2(*d*) ordered sites (in $P6_3/mmc$ notation) – later known as the Beevers–Ross (BR) sites. In these sites, the Na^+ ions coordinate to six O atoms in the spinel block. The somewhat smaller vacant 2(*b*) sites were consequently referred to as anti-Beevers–Ross (aBR) sites, where O atoms are found immediately above and below the site. It was later argued by Saalfeld (1956) that Na^+ β-alumina is non-stoichiometric. Phase analysis studies by Weber & Vereno (1969) suggested a non-stoichiometry with a 15–30% excess of sodium. A fresh structural determination (Peters, Bettman, Moore & Glick, 1971) resulted in the composition $Na_{1{\cdot}29}Al_{10{\cdot}9}O_{17}$, with a more complex Na^+-ion distribution. They also proposed that the sodium-ion excess was compensated for by vacancies among the aluminium ions in the spinel block. A later study by Reidinger (1979) using neutron diffraction showed that the excess of sodium ions was not, in fact, compensated for by Al vacancies, but rather by extra oxygen in the conduction plane. These oxygens were stabilized by interstitial aluminium ions becoming displaced from their normal sites in the spinel block forming a Frenkel defect. Reidinger's work has never appeared in any readily accessible form, however.

Theoretical methods have also been used in the study of conduction mechanisms and ionic distribu-

0108-7681/91/020210-07$03.00 © 1991 International Union of Crystallography

tions within these types of materials. In a molecular dynamics (MD) simulation of Na^+ β-alumina (Zendejas & Thomas, 1990), Newton's equations of motion were solved simultaneously for ions in a simulation box involving $3 \times 3 \times 1$ crystallographic unit cells. Their calculations suggest a slightly different distribution of Na^+ ions in the conduction plane from that found in the experiments described here. Instead of the two Na^+-ion sites of Reidinger, three distinct sites appear. The question thus arises as to whether this discrepancy arises from inadequacies in the theoretical treatment or is, indeed, real and can be supported by a careful diffraction experiment.

Despite all previous work, there is therefore a clear need for a definitive structural study using modern crystallographic refinement techniques. Any proposed conductivity mechanism must be consistent with the observed (albeit overlapped) total Na^+ distribution. In the knowledge that earlier studies have shown the Na^+-ion distribution to be considerably extended in space, it is thus of fundamental interest also to explore the use of the diffraction techniques in studying this type of dynamically disordered situation. We invoke conventional single-crystal X-ray diffraction techniques and ascertain the extent to which the Na^+-ion distribution can be described satisfactorily by the models we have at our disposal.

Experimental

Na^+ β-alumina single crystals were obtained from Union Carbide Corporation. The crystal used (maximum/minimum dimensions: 0·220/0·133 mm) was cracked from a larger piece. The crystal dimensions and orientation matrix have been deposited.* The composition, $Na_{1\cdot22}Al_{11}O_{17\cdot11}$, given by Union Carbide agreed well with our experimental measurements of the linear absorption coefficient μ on the larger crystal. Crystal quality was checked with Laue films, and the intensities measured at 295 K with an Enraf–Nonius CAD-4 automatic diffractometer controlled by a PDP8/A computer. Integrated intensities measured using an $\omega/2\theta$ step scan (96 steps). Data were collected up to $\sin\theta/\lambda = 1\cdot09$ Å^{-1} for $0 \le h \le 10$, $0 \le k \le 10$, $0 \le l \le 48$. Each intensity was measured three times at 0·5° intervals in ψ as a means of detecting multiple reflections. 7575 intensities were collected, 83 were remeasured following discrepancies in the triplets or uneven background. After averaging triplets, 2525 reflections remained giving 1246 unique reflections; $R_{\rm int} = \sum|I_o - \bar{I}_o|/\sum I_o = 0\cdot023$ after merging equivalent reflections, though refinements were based on the unmerged data set. Intensity data were corrected for background (Lehmann & Larsen, 1974), and five standard reflections with the indices 220, 034, $\bar{4}$,0,$\bar{1}\bar{3}$, 2,0,13 and 0,2,14 within a variation of 4%, were used to scale intensities and standard deviations (McCandlish, Stout & Andrews, 1975). Lp and absorption corrections were applied. A linear absorption coefficient was measured experimentally and used in the absorption correction, which also employed an explicit description of the crystal size and shape. The transmission-factor range was 0·82–0·88. Cell parameters were determined from a least-squares fit to observed 2θ angles for 25 reflections in the range $22 < 2\theta < 45°$, measured prior to the data collection. Systematic absences indicated the possible space groups $P6_3/mmc$ and $P6_3mc$. Both were tested in the refinements, which were made using the full-matrix least-squares refinement program *DUPALS* on a departmental microVAX II. The function minimized was $\sum w(|F_o|^2 - |F_c|^2)^2$, where $w^{-1} = \sigma^2(F_o^2) = \sigma_c^2(F_o^2) + (kF_o^2)^2$; k is an empirical constant set to 0·01. Reflections for which F_o^2 was less than $2\sigma(F_o^2)$ were removed from the refinement (see Table 1). Anomalous-dispersion terms and coherent-scattering amplitudes used for Al^{3+}, O^{2-} and Na^+ were those taken from *International Tables for X-ray Crystallography* (1974, Vol. IV). All computer programs have been described by Lundgren (1982).

Table 1. *Agreement factors for the final four refined models*

Refinement	Model refined	No. of parameters refined	$R(F)$	$R(F^2)$	$wR(F^2)$	No. of reflections
(1)	The Na^+ ions in the 2(*d*) site refined (β_{ij} and γ_{ijk} tensors)	46	0·0187	0·0240	0·0436	2036
(2)	Na(1) refined in split-atom 6(*h*) site (β_{ij}'s)	47	0·0188	0·0243	0·0445	2036
(3)	Noncentrosymmetric $P6_3mc$; Na(1) and Na(2) at 6(*c*) sites (β_{ij}'s)	52	0·0183	0·0236	0·0430	2036
(4)	Na^+-ion sites and occupations from MD simulation, only thermal parameters (β_{ij}'s) refined for Na^+ ions	46	0·0219	0·0282	0·0567	2036

The refinements

The starting parameters for the structural description of the spinel-block atoms were taken from Peters *et al.* (1971). A first crude picture of the Na^+-ion distribution in the conduction plane was obtained from a difference Fourier synthesis calculated after an initial refinement of the spinel-block structure. The Na^+-ion distribution is seen to have a maximum at a 2(*d*) site (hereafter referred to as a BR

* The crystal size and shape, and lists of harmonic and anharmonic atomic displacement parameters, interatomic distances and structure factors have been deposited with the British Library Document Supply Centre as Supplementary Publication No. SUP 53647 (27 pp.). Copies may be obtained through The Technical Editor, International Union of Crystallography, 5 Abbey Square, Chester CH1 2HU, England.

site), with a significant trigonal distortion in the direction of the conduction pathways. Na^+ ions were included in the model at BR sites and their occupations refined. On the basis of a subsequent difference Fourier synthesis, a second Na^+ ion was then added at an interstitial 6(*h*) site, referred to as an *A* site, and its occupation also refined. Large correlation effects between site-occupation and thermal-displacement parameters necessitated the constraint of occupation parameters to the expected sodium content.

The observed trigonal distortion around the BR site was modelled in two different ways. The Na^+ ions were first shifted out to 6(*h*) sites (at $x, -x, z$) in combination with anisotropic displacement parameters (β_{ij}'s). A second approach was to place the Na^+ ions at the BR site and refine both second- and third-order cumulants (β_{ij}'s and γ_{ijk}'s) (*International Tables for Crystallography*, 1974, Vol. IV) (Figs. 2*a* and 2*b*). The agreement factors obtained from these two refinements were almost identical (Table 1; refinements 1 and 2).

In both models, the compensating oxygen ion in the Roth–Reidinger defect, O(6), was located at a 6(*h*) site (the mO site) exactly between the column oxygens O(5). The interstitial aluminium ions, Al(5), were found in difference maps at $z \simeq 0{\cdot}175$ and $z \simeq 0{\cdot}325$, and their positional parameters refined. Their anisotropic displacement parameters were constrained to the values of Al(1). For the best fit

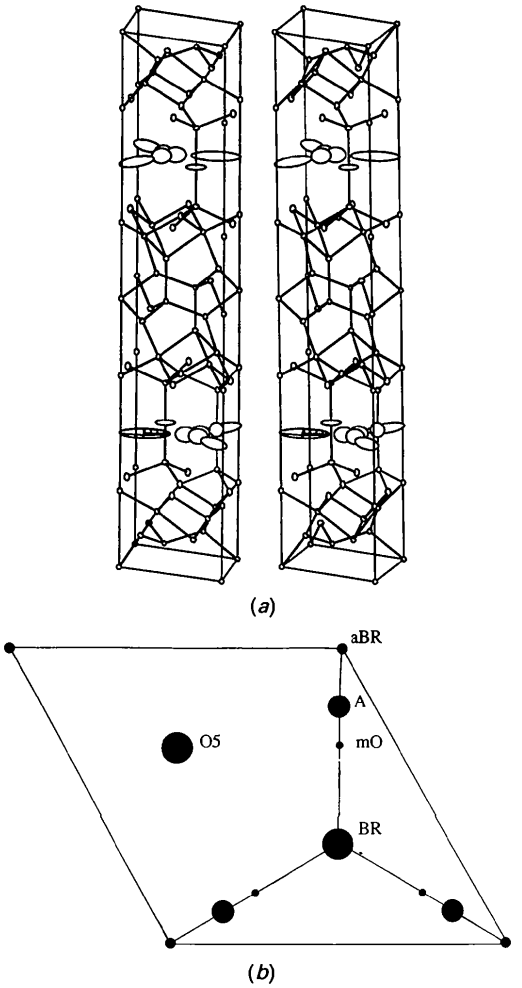

Fig. 1. (*a*) A stereoscopic *ORTEP* picture of the structure of Na^+ β-alumina. (*b*) A schematic representation of sites available for Na^+-ion occupation within the $z = \frac{1}{4}$ conduction plane. The sizes of the atoms are scaled to the relative occupations of the BR and *A* sites.

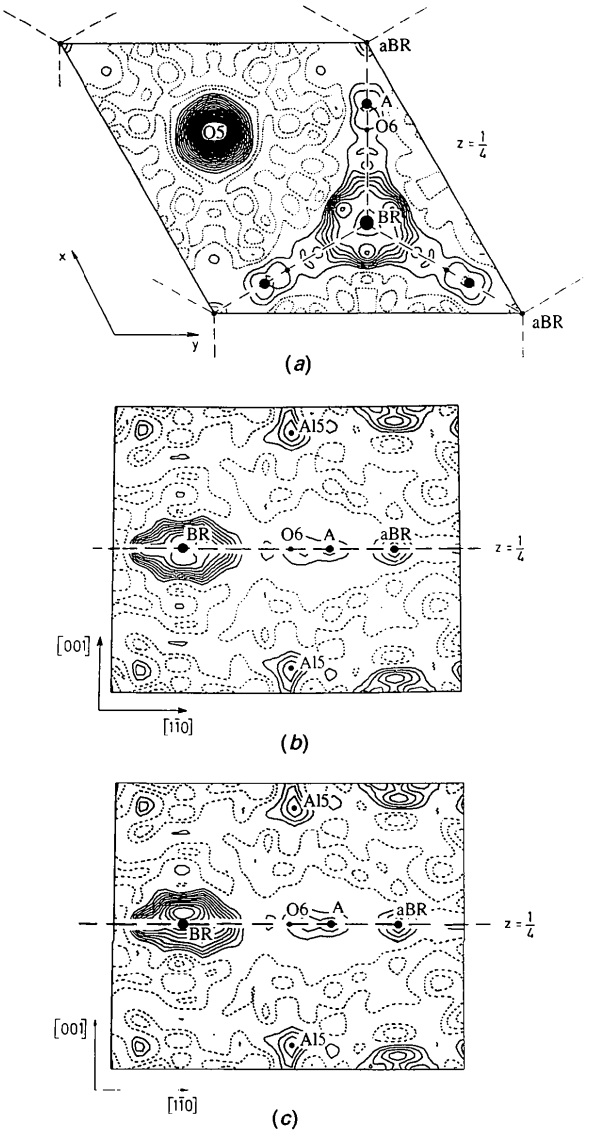

Fig. 2. Observed Fourier syntheses for Na^+ β-alumina in: (*a*) the conduction plane at $z = \frac{1}{4}$; (*b*) the $(x, -x, z)$ plane and (*c*) the $(x, -x, z)$ plane, using space group $P6_3mc$. All contour intervals are $0{\cdot}7$ e $Å^{-3}$.

Table 2. *Atomic positional parameters* ($\times 10^5$), *equivalent isotropic displacement parameters for the spinel block (expressed as mean r.m.s amplitudes,* $U_{eq} \times 10^3$) *and anisotropic displacement parameters* ($\beta_{ij} \times 10^4$) *for the* Na^+ *ions and the* O(5) *atoms in* Na^+ *β-alumina (see Table* 1, *refinement* 5)

$$U_{eq} = (U_{11} + U_{22} + U_{33})/3.$$

	Site	Occupation	x	y	z	β_{11} or U_{eq} (Å^2)	β_{22}	β_{33}	β_{12}	β_{13}	β_{23}
Na(1)	2(*d*)*	0·734 (4)	$\frac{2}{3}$	$\frac{1}{3}$	$\frac{1}{4}$	1229 (16)	β_{11}	14·9 (4)	$\beta_{11}/2$	0	0
Na(2)	6(*h*)	0·162 (4) (× 3)	89702 (130)	$-x$	$\frac{1}{4}$	1338 (34)	β_{11}	3·9 (4)	−400 (48)	0	0
O(5)	2(*c*)		$\frac{1}{3}$	$\frac{2}{3}$	$\frac{1}{4}$	660 (6)	β_{11}	0·93 (10)	$\beta_{11}/2$	0	0
Al(1)	12(*k*)	0·963	−16798 (1)	$2x$	10610 (1)	4·9					
Al(2)	4(*f*)		$\frac{1}{3}$	$\frac{2}{3}$	2482 (1)	3·8					
Al(3)	4(*f*)		$\frac{1}{3}$	$\frac{2}{3}$	17576 (1)	6·1					
Al(4)	2(*a*)		0	0	0	4·3					
O(1)	12(*k*)		15712 (2)	$2x$	4998 (1)	5·1					
O(2)	12(*k*)		50305 (2)	$-x$	14632 (1)	6·2					
O(3)	4(*f*)		$\frac{2}{3}$	$\frac{1}{3}$	5525 (2)	5·2					
O(4)	4(*e*)		0	0	14219 (2)	4·7					
Al(5)	12(*k*)	0·037	−16045 (5)	$2x$	17523 (12)	4·9					
O(6)	6(*h*)	0·037	$\frac{5}{6}$	$\frac{1}{6}$	$\frac{1}{4}$	38·0					

* Refined values for third-order cumulants (γ_{ijk} in Å^3) for Na(1): γ_{111} ($= -\gamma_{222} = 2\gamma_{112} = -2\gamma_{122}$) = −0·166 (5); $\gamma_{333} = \gamma_{113} = \gamma_{133} = \gamma_{223} = \gamma_{233} = \gamma_{123} = 0$.

(refinement 1 in Table 1), maximum/minimum values in final difference Fourier maps were 0·72/−1·06 e Å^{-3}, $S = 2{\cdot}57$, $(\Delta/\sigma)_{max} = 0{\cdot}1$. Note, however, that these unusually large peaks merely serve to focus on the special problems involved in modelling this type of system.

A further approach can be taken in probing the nature of the local ordering between Na^+ ions. We can lower the effective space-group symmetry for the mobile ions but retain the higher symmetry for the spinel block. This has earlier proved rewarding for the divalent β″-aluminas (Thomas, Aldén, McIntyre & Farrington, 1984) but has not been used previously for the β-aluminas. It was now tested for the Na^+ ions and for the Frenkel defect. There are serveral ways in which the effective symmetry can be lowered. We have here chosen to remove the mirror planes at $z = \frac{1}{4}$ and $z = \frac{3}{4}$. In this way, refinement should expose local order in the ionic arrangement. It is also possible that the interstitial aluminium ions, Al(5), occur locally on only one side of the mirror plane; the validity of the mirror symmetry in the Frenkel defect was therefore also tested in this way. The effective space group used for the Na^+ ions and atoms in the Roth–Reidinger defect was non-centrosymmetric $P6_3mc$ (see Table 1; refinement 3 and Fig. 2*c*).

In the MD simulation referred to earlier for a 3 × 3 × 1 simulation box of Na^+ β-alumina (Zendejas & Thomas, 1990), of the 11 Na^+ ions in the box, one occupied an aBR site, two occupied *A*-type sites, and the remaining eight were found at or near BR sites. This model was tested by placing 1/11 of the 1·22 Na^+ ions per cell layer in the aBR site, 2/11 at the MD-determined *A* sites, and 8/11 at split-atom sites close to the BR site; β_{ij} tensors were refined but occupations and positional parameters fixed for all Na^+ ions (see Table 1; refinement 4).

Results and discussion

The structure

The structure comprises Al atoms octahedrally and tetrahedrally coordinated by O atoms to form spinel layers separated in the **c** direction by Al(3)—O(5)—Al(3) bridging bonds (Fig. 1). The 'conduction planes' (at $z = \frac{1}{4}$ and $z = \frac{3}{4}$) only contain the column-oxygen ions, O(5), the mobile Na^+ ions, and (in roughly 10% of the layers) the extra oxygen, O(6). The Na^+ ions are distributed along edge-linked hexagonal pathways around the O(5) atoms. The BR and aBR sites represent the junctions in the conduction pathways, with the space available at BR sites somewhat greater than at aBR sites, which favours the occupation of Na^+ ions in BR sites. Indeed, they are found at the BR and *A* sites with aBR sites essentially empty. The O(5) atom occupies a 2(*c*) site. The extra oxygen ions occupy mO sites and are bonded to the spinel block *via* interstitial aluminium ions, Al(5), at $z \simeq 0{\cdot}175$ and $z \simeq 0{\cdot}325$. These are displaced from the Al(1) site (see Fig. 1), such that the occupation of Al(1) is diminished by an amount corresponding to the Al(5) occupation. This is the Roth–Reidinger defect which compensates the sodium-ion excess in the conduction plane (Roth, Reidinger & LaPlaca, 1976; Reidinger, 1979), and which is characteristic of the β-alumina structure. Though permitting extra Na^+ ions in the conduction planes, the Roth–Reidinger defect also decreases ionic conductivity by effectively blocking some of the pathways and forming a local trap for its nearest Na^+ ions. Refined positional and thermal parameters are found in Table 2.*

A refined model for the conduction plane gives the unit-cell time- and space-averaged picture of its ionic

* See deposition footnote.

distribution. The refinement of an averaged electron density for an extended ionic distribution of this type is handicapped by the lack of a convenient mathematical formalism for this purpose. The resulting 'structure' thus comprises an average cell content involving partially occupied atom sites. This result is essentially unphysical, but can nevertheless be used to gain some indication of likely local ionic arrangements.

There are several compromises we can make in describing the average electron density. We can use 'split-atom' sites, whereby a given ion site, which is at a charge distribution centroid, is replaced by two or more sites of lower symmetry. Another possible model invokes anisotropic displacement parameters of higher rank. Typically, a Gram–Charlier expansion model can be used to modify the harmonic anisotropic displacement parameters such that the general structure factor will be:

$$F(\mathbf{h}) = \sum_{j=1}^{N} f_j \exp\left(\sum_{k=1}^{3} \left\{ 2\pi i h_k x_k^j - \sum_{l=1}^{3} \left[h_k h_l \beta_{kl}^j \left(1 - \sum_{m=1}^{3} i h_k h_l h_m \gamma_{klm}^j \right) \right] \right\} \right)$$

where β_{ij} and γ_{ijk} are tensor terms of rank 2 and 3, and N is the number of atoms in the unit cell (*International Tables for X-ray Crystallography*, 1974, Vol. IV; Prince, 1982). The existence of non-zero values for the third-order cumulants may be used in principle as a measure of anharmonicity in interaction potentials or of positional disorder. It should be noted, however, that these higher-rank tensor terms are frequently involved in extremely large correlations (often > 90%). This makes any qualitative interpretation of their individual values highly questionable. Tensors of up to rank 4 (β's, γ's and δ's) have been used for the thermal description of the divalent β''-aluminas (Aldén, 1985) and appear to give a satisfactory description of the average distribution. The present study shows that no one model is favoured over any other. The higher-cumulant model gives slightly better agreement factors, while the split-atom models are perhaps more physical (Table 1; refinements 1 and 2, Figs. 2*a* and 2*b*).

None of these models succeeds in describing the form of the average electron distribution observed around the BR site in sections perpendicular to the conduction plane (Fig. 2*b*). This map can be interpreted as implying a residual electron density maximum outside the conduction plane. Models involving Na^+ ions shifted away from the conduction plane (in the **z** direction) were tested in several ways, *viz.* the Na^+ ion at the BR site was shifted out from the plane, or the electron distribution was separated into two or three Na^+-ion positions around the BR site. Neither model improved the agreement significantly.

We have so far discussed the use of a conventional refinement procedure in which we impose the symmetry of the majority of the structure (here the spinel-block host) onto a minority component (here the mobile ions) which, from stoichiometric considerations, cannot possibly share this symmetry locally. A more rational approach would be to use a lower symmetry for the mobile ions. This was tested by the removal of the mirror operation in the conduction plane through the use of the space group $P6_3mc$. No significant improvement was obtained (see Table 1 and Fig. 2*c*). The occupation of the aluminium atoms, Al(5), was also refined to probe the validity of the mirror plane in the Roth–Reidinger defect. Again, no effective lowering of symmetry could be established.

The role of the Roth–Reidinger defect

It has been postulated that the mechanism for Na^+-ion mobility is based upon correlated Na^+-ion pairs occurring at interstitial sites (here *A* sites) (Whittingham & Huggins, 1971). On the discovery of the Roth–Reidinger defect (Roth *et al.*, 1976; Reidinger, 1979), it was realized that this mechanism was too simplistic, and that the extra O(6) atom must play an important role.

Inspection of refined Na^+-site occupations (0·73 of the 1·22 Na^+ ions in a unit cell layer are in BR sites; 0·49 in *A*-type sites) can give some notion as to how Na^+-ion mobility may occur. It has been suggested that a structurization of Na^+ ions occurs around the O(6) atom (Roth, Reidinger & LaPlaca, 1976; Redinger, 1979). Interpreting our result, this local arrangement consists of Na^+ ions in *A*-type sites around the O(6) atom, such that the Na^+ ions closest to O(6) will have an Na^+—O distance of 2·283 (6) Å: somewhat longer than the Na^+—O distance in Na_2O (~2·16 Å). This ion is found on the aBR side of the O(6) atom, see Fig. 4. The next-closest *A* site is 3·345 (6) Å away from the O(6) atom, on the BR side of O(6) (Fig. 4). On this side, two Na^+ ions can occupy two *A* sites simultaneously; on the other side, this is not possible due to the short *A*—*A* distance. The diffraction result corresponds to four ions in *A* sites and seven ions in BR sites in a 3 × 3 cell. A fourth *A*-site ion is therefore also produced by the Roth–Reidinger defect and can be seen in Fig. 4. A similar complex has been suggested by Roth *et al.* (1976) and Reidinger (1979) but with the four Na^+ ions found in mO sites. Calculations based on the Haven ratio for several configurations have shown Roth–Reidinger's model to be the most energetically favourable. At higher temperatures, it is suggested that the Na^+ ions in mO

sites become thermally activated and involved in the conductivity process (Wolf, 1979). The local structurization of Na^+ ions around O(6) involves up to four *A*-site ions and one BR ion (Fig. 4). No direct conclusions can be drawn on the basis of our X-ray diffraction experiment concerning the nature of the conduction mechanism, however. We cannot state that one ion is more mobile than another; nor can we do more than speculate on possible dynamical correlations which may exist. On the other hand, we can probe these aspects through the exchange of Cd^{2+} ions into the Na^+ β-alumina host (Edström, Thomas & Farrington, 1991).

Studies of the local arrangement of Na^+ ions around the O(6) atom have also been made using other techniques; an NMR study at 5 K (Carduner & White, 1986) has shown, for example, that the O(6) atom is surrounded by Na^+ ions which occupy two slightly different site types [one somewhat closer to O(6) than the other], with relative occupations 8·5 and 25·5%. This same type of arrangement has been proposed from potential-energy calculations (Wang, 1980). This picture is in no way contradicted by our diffraction result. Rather, it contains more subtle detail concerning the Na^+ distribution which our diffraction study is unable to expose.

The Na^+-ion distribution from an MD simulation (Zendejas & Thomas, 1990) results in an ionic distribution in the conduction plane which differs qualitatively from our best refined model (experiment: 2/3 of the Na^+ ions in BR sites and 1/3 in *A* sites; MD: 8/11 in BR sites, 2/11 at *A* sites and 1/11 in aBR sites). Another type of local structurization around O(6) is proposed whereby two Na^+ ions are found in BR sites on one side of the O(6) atoms, and two at *A* sites are on the other; one ion is found in the aBR site, and the rest in the BR sites. The Na^+ ions in the local structurization appear to be rather stable, with the mobility occurring outside the structurized region. The conductivity is induced by the ion in the aBR site. Only at high temperatures does the local influence of the O(6) atom disappear. This result clearly contradicts the earlier picture that Na^+ ions around O(6) are those involved in the conduction mechanism. This MD picture may be spurious, resulting from the use of too small a simulation box or of inappropriate pair potentials. Alternatively, we know that our diffraction experiment has great difficulty in resolving the overlapped Na^+ distribution. A test was made in which the thermal parameters in the MD model were refined. This resulted in poorer agreement (Table 1, refinement 4), although it may be noted that an F_c synthesis based on this model (Fig. 3*a*) closely resembled the F_o synthesis

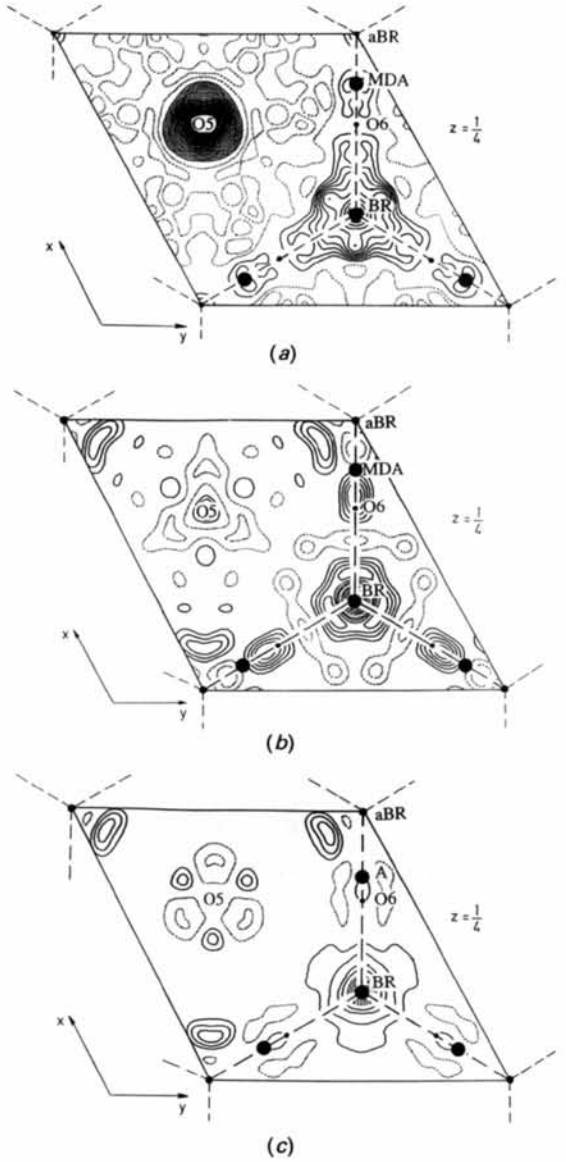

Fig. 3. Comparison between experimental and theoretical (MD simulated) Na^+-ion distributions in Na^+ β-alumina. (*a*) F_c synthesis for MD simulated model; contour interval 0·7 e Å^{-3}. (*b*) $(F_o - F_c)$ difference synthesis for the MD simulated model; contour interval 0·2 e Å^{-3}. (*c*) $(F_o - F_c)$ difference synthesis for the experimental result; contour interval 0·2 e Å^{-3}.

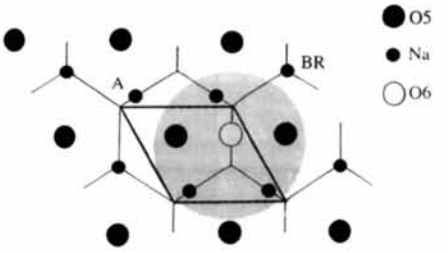

Fig. 4. The sphere of greatest influence for the charge compensating O(6) atom.

Table 3. *Some interatomic distances* (Å) *in* Na^+ *β-alumina*

		Mean
Na(1)—O(2) (×6)	2·822 (1)	
Na(1)—O(5) (×3)	3·229 (1)	
Na(2)—O(6) (×2)	2·283 (6)	
Na(2)—O(4) (×2)	2·626 (2)	
Na(2)—O(5) (×2)	2·864 (6)	
Na(2)—O(6) (×2)	3·345 (6)	
Al(1)—O(4) (×1)	1·819 (1)	1·916 (10)
Al(1)—O(2) (×2)	1·833 (1)	
Al(1)—O(3) (×1)	1·969 (1)	
Al(1)—O(1) (×2)	2·021 (1)	
Al(2)—O(1) (×3)	1·799 (1)	1·801 (2)
Al(2)—O(3) (×1)	1·804 (1)	
Al(3)—O(5) (×1)	1·672 (1)	1·7489 (10)
Al(3)—O(2) (×3)	1·773 (1)	
Al(4)—O(1) (×6)	1·893 (1)	1·893
Al(5)—O(6) (×1)	1·685 (3)	1·731 (30)
Al(5)—O(4) (×1)	1·723 (1)	
Al(5)—O(2) (×2)	1·757 (1)	

arising from refinement 1 (Fig. 2*a*). On the other hand, a difference synthesis between our data and the MD model contains significant residual density in the mO-site region (Fig. 3*c*). In this connection, it is significant to note that the refined model gives *A*-site positions ~0·2 Å closer to mO than the MD simulation, and no aBR-site occupation.

The column-oxygen atoms, O(5), are suggested by the MD simulation to be displaced away from their normal 2(*c*) positions under the repulsion they experience from the O(6) atom. This behaviour is supported by our results in which unusually large thermal-displacement parameters are refined for O(5) in the conduction plane and small values in the **z** direction (Table 3).

Concluding remarks

Three refined models (Table 1; refinements 1 to 3) are found to describe the Na^+ distribution almost equally well. In the sense that all such models are equally unphysical, they should perhaps all be regarded as equally inappropriate in describing the real Na^+-ion distribution. The main problem however is that no simple method exists for describing an extended disorder phenomenon of this type. Nevertheless, apart from highlighting the experimental difficulties inherent in studying this type of material, we believe such investigations, in combination with MD simulation, do help in arriving at some understanding of local conduction mechanisms.

This research has been supported in part by the Swedish Natural Science Research Council (NFR), and in part by the United States Office of Naval Research under Contract No. N00014-81-K-0526. We are also most grateful to our laboratory technician Hilding Karlsson for his skilled assistance.

References

ALDÉN, M. (1985). *Acta Universitatis Upsaliensis*. Comprehensive summaries of Uppsala Dissertations from the Faculty of Science, 3.

BEEVERS, C. A. & ROSS, M. A. S. (1937). *Z. Kristallogr.* **97**, 59–66.

BRAGG, W. L., GOTTFRIED, C. & WEST, J. (1931). *Z. Kristallogr.* **77**, 255–274.

CARDUNER, K. R. & WHITE, D. (1986). *J. Chem. Phys.* **85**, 3173–3179.

EDSTRÖM, K., THOMAS, J. O. & FARRINGTON, G. C. (1991). *Acta Cryst.* **B47**. Submitted.

LEHMANN, M. S. & LARSEN, F. K. (1974). *Acta Cryst.* **A30**, 580–584.

LUNDGREN, J.-O. (1982). *Crystallographic Computer Programs*. Report UUIC-B13-04-05. Institute of Chemistry, Univ. of Uppsala, Sweden.

MCCANDLISH, L. E., STOUT, G. H. & ANDREWS, L. C. (1975). *Acta Cryst.* **A31**, 245–249.

PETERS, C. R., BETTMAN, M., MOORE, J. W. & GLICK, M. D. (1971). *Acta Cryst.* **B27**, 1826–1834.

PRINCE, E. (1982). *Mathematical Techniques in Crystallography and Materials Science*. New York: Springer-Verlag.

REIDINGER, F. (1979). PhD Thesis, State Univ. of New York, Albany, USA.

ROTH, W. L., REIDINGER, F. & LAPLACA, S. (1976). *Superionic Conductors*, edited by G. D. MAHAN & W. L. ROTH, pp. 223–241. New York: Plenum Press.

SAALFELD, H. (1956). *Z. Anorg. Allg. Chem.* **286**, 174–179.

THOMAS, J. O., ALDÉN, M., MCINTYRE, G. J. & FARRINGTON, G. C. (1984). *Acta Cryst.* **B40**, 208–213.

WANG, J. C. (1980). *J. Chem. Phys.* **73**, 5786–5795.

WEBER, N. & VENERO, A. F. (1969). Publication preprint SR69-102, Ford Motor Co.

WHITTINGHAM, M. S. & HUGGINS, R. A. (1971). *J. Electrochem. Soc.* **118**, 1.

WOLF, D. (1979). *J. Phys. Chem. Solids.* **40**, 757–773.

YAO, Y. F. & KUMMER, J. T. (1967). *J. Inorg. Nucl. Chem.* **29**, 2453–2474.

ZENDEJAS, M. A. & THOMAS, J. O. (1990). *Phys. Scr.* In the press.